Geomech. Geophys. Geo-energ. Geo-resour. (2023) 9:163
https://doi.org/10.1007/s40948-023-00697-y

RESEARCH

Study on the fault slip rule and the rockburst mechanism induced by mining the panel through fault

Peng Kong · Changxiang Wang · Luyi Xing · Min Liang · Jin He

Received: 29 July 2023 / Accepted: 19 November 2023

Abstract When mining near the fault can cause the fault to slip and release energy, resulting in rockburst and posing a significant safety risk to coal mine production. This paper proposes a numerical simulation method, based on FLAC3D numerical simulation, for calculating the dynamic response of fault slip below the impact of mining. The release patterns of energy from fault slip are compared between mining via the fault from the hanging wall and mining via the fault from the footwall. The dynamic response characteristics of coal and rock mass under the disturbance of fault slip induced dynamic loading are revealed. This research suggests that the fault slip seismic moment (M_0) of the panel mined via the fault from footwall is substantially higher than from hanging wall. Moreover, the disturbance of the footwall panel mining via the fault leads to a more severe disturbance of the surrounding rock mass, resulting in a higher risk of rockburst. Plastic failure of the rock surrounded in the mining area under the strong dynamic loading of fault slip leads to a significant reduction in peak abutment stress, releasing tremendous energy. When the disturbance caused by fault slip dynamic load is relatively small, the maximum abutment stress increases, and the dynamic load increases the energy storage of surrounding rock. Based on energy theory, an energy criterion for the occurrence of fault slip type rockburst has been proposed. The results suggest that strong fault slip dynamic load has an obvious inducing effect on rockburst, and the stronger the dynamic load and greater static load of the rock, the more the manifestation of rockburst.

P. Kong · C. Wang (✉) · J. He
Engineering Laboratory for Safe and Precise Coal Mining of Anhui Province, Anhui University of Science and Technology, Huainan 232000, China
e-mail: 1554624100@qq.com

C. Wang
School of Safety Science and Engineering, Anhui University of Science and Technology, Huainan 232000, China

L. Xing
Shandong Key Laboratory of Civil Engineering Disaster Prevention and Mitigation, Shandong University of Science and Technology, Qingdao 266590, China

L. Xing (✉)
School of Civil Engineering, Shandong Jianzhu University, Jinan 250101, China
e-mail: xingluyi20@sdjzu.edu.cn

M. Liang
Land Spatial Data and Remote Sensing Technology Institute of Shandong Province, Jinan 250002, China

Article Highlights

- Based on FLAC3D numerical simulation, a dynamic calculation method for fault slip under mining influence was proposed. The release patterns of energy from fault slip are compared between mining via the fault from the hanging

Published online: 07 December 2023

wall and mining via the fault from the footwall. The dynamic response characteristics of coal and rock mass under the disturbance of fault slip induced dynamic loading were revealed.

- Compared with mining the panel via the fault from hanging wall, the fault released more energyM($_0$) when mining the panel via the fault from footwall, resulting in a higher vibration velocity of the surrounding rock in the mining area and a higher possibility of rockburst.
- Based on energy theory, an energy criterion for the prevalence of fault slip type rockburst was proposed. The initiation and severity of fault slip rockburst are closely related to the magnitude of the energy released by fault slip and the static stress of surrounding rock. The potential of rockburst was higher under the combined effect of high static stress and dynamic load of fault slip.

Keywords Rockburst · Fault slip · Dynamic response · Energy

1 Introduction

As the depth of exploitation of coal increasing and the continuous deterioration of geological prerequisites in mines, rockbursts occur frequently and haveend up one of the essential mess ups that impede secure and environment friendly coal mining. Production practices has indicate that 70% of rockburst accidents occur near fault structures. Moreover, compared with roof fracture type and coal pillar instability type rockbursts, fault slip type rockbursts possess the characteristics of a complex triggering mechanism, a large impact range, and more severe rockburst manifestation (Mottahedi et al. 2019, Vardar et al. 2022, Fan et al. 2019, Jiang et al. 2019).

Here are two stages in in technique of fault slip kind rockbursts. The first one is the fault slip activation and launch massive quantity of electricity below the effect of mining, which can be called the fault slip stage. The second stage is that the energy propagates from fault slip in the form of dynamic loading stress waves, acting on the mass of coal-rock in the mining area. Under the combined action of Dynamic loads together with the static loads make the mass of coal-rock in the mining area experience instability and failure, ultimately leading to the manifestation of dynamic pressure. This stage can be called the stage of rockburst manifestation.

In terms of the activation law of fault slip under mining influence, Wang et al. (2021) used theoretical analysis to calculate the normal stress and shear stress of faults under the influence of mining, and proposed the concept of fault potential energy to evaluate the energy stored by faults and reveal the mechanism of fault sliding. Scholars (Xiao et al. 2023, Cai et al. 2021, Avuli et al. 2021) have used microseismic monitoring methods to monitor the activation characteristics of faults during mining. In the advancement of working face near the fault, the frequency as well as depth of microseismic activities in the vicinity affected by fault considerably increase, and there is a clear zoning or cluster strip distribution of microseismic occasions close to the fault which is indicated to undergo slip and release energy due to slip. Wang et al. (2014) conducted similar simulation experiments on working face mining to investigate how mining influences the rule of fault slip. It was put forward that on the fault plane, the magnitude of normal stress is crucial in determining fault closure or slip. Kong et al. (2019) conducted research on the evolution of fault stress under mining influence using numerical simulation and proposed a fault slip potential index to evaluate the hazard of fault slip.

In terms of the rockburst manifestation of stope surrounding rock under the combined action of dynamic and static loads, Su et al. (2021) conducted experimental research on the dynamic characteristics of underground excavation under the combined action of dynamic and static loads. The research showed that the strength of rockburst is not only related to the magnitude of static load, but also influenced by the type and characteristics of dynamic load disturbance. Hu et al. (2018) conducted a true triaxial dynamic static coupling experiment to study the crack propagation and energy dissipation characteristics of rock samples under tangential dynamic load disturbance. The study showed that weak dynamic disturbance accelerated the extension of tensile cracks, thereby triggering the occurrence of rockburst. Wang et al. (2018) analyzed the generation mechanism of dynamic load stress wave in stope and studied the rules of coal-rock mass destruction under various dynamic and dynamic loading conditions. It is considered that rockburst is the result of coupling effect between static and dynamic stress waves and coal rock mass structure. Chen et al. (2016) studied the dynamic response characteristics of roadway surrounding rock under different focal mechanisms using numerical simulation, and the research showed that the peak particle velocity (PPV) of rock mass in the S-wave radiation quadrant was significantly greater than that one in the P-wave radiation quadrant.

Scholars have researched under mining the rule of fault slip and the mechanism of impact instability of coal rock body influenced by both static loads and dynamic loads. However, the relationship between working face layout and mining direction and fault is complicated, and there is no quantitative study on the magnitude of fault slip energy release under different mining influences. In particular, there is a lack of comparative analysis on the energy release characteristics of fault slip when the working face traverses the fault from the footwall and hanging wall sides. Consequently, it is difficult to accurately evaluate the the dynamic response characteristics and impact hazard of coal rock body in mining space. This paper also investigates the dynamic response characteristics of coal rock loads below fault slip disturbance, and proposes an energy criterion for rockburst instability under static and dynamic loading. The research findings are significant to reveal the inducing mechanism of fault slip type rockburst and propose a rockburst instability energy criterion with static and dynamic loading to predict fault slip type rockburst.

2 Engineering background

Dongtan Coal Mine is situated in the city of Jining, Shandong Province, China. The coal seam in Panel 14,310 has 8 m in the average thickness, meanwhile it is mined using near-horizontal mining. The working face is 230 m long with an advancing length of 2000 m, and and the panel geological stipulations are complicated. The inclination angle of the is 60° and a vertical displacement is 6 ~ 10 m. Figure 1 shows the layout and fault location of Panel 14,310, while Fig. 2 shows the rock stratum histogram. The working face passes over the fault from the footwall side during mining operations, and strength degree of microseismic occasions appreciably make bigger all through the mining period. Moreover, almost all the microseismic events with large energy occurr near faults, and the mining pressure in the stope is more severe under the strong microseismic activity caused by fault slip (Kong et al. 2022).

Fig. 1 Plan of the panel

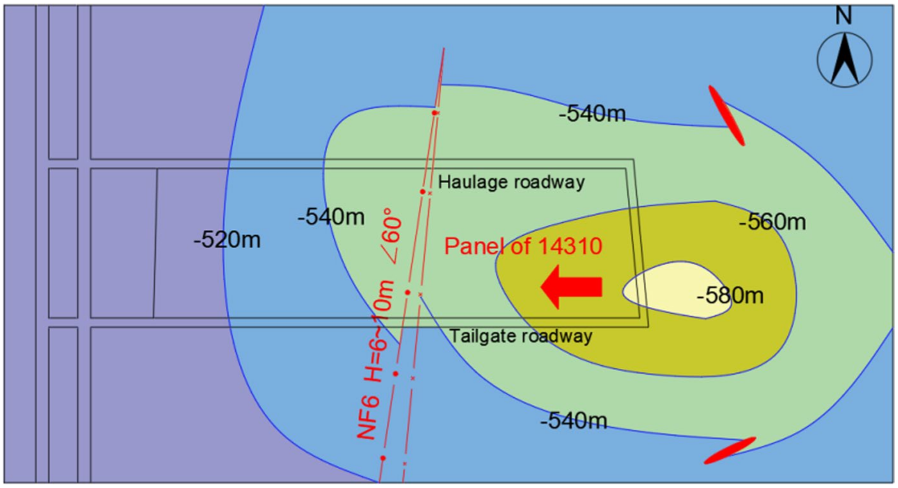

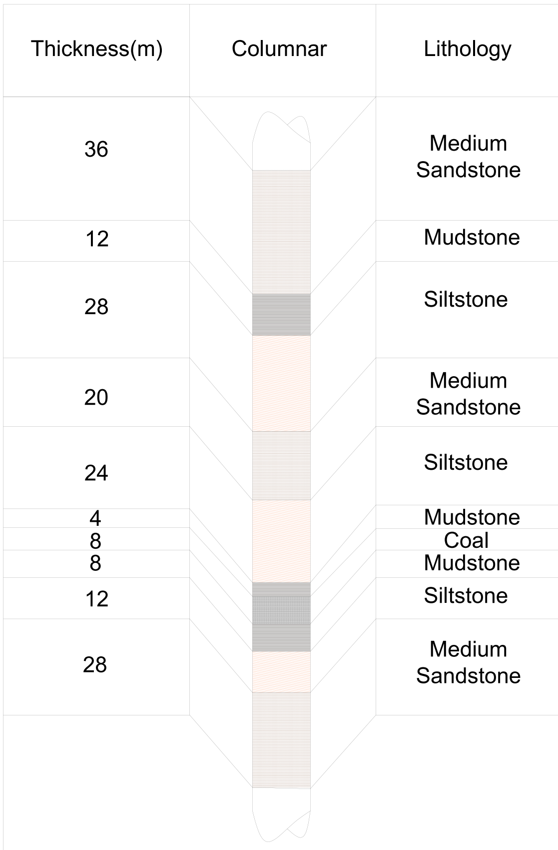

Fig. 2 Column diagram of the panel

3 Numerical simulation analysis

3.1 Model model setup

Based on the formation conditions of Panel 14,310 in Dongtan Coal Mine and the characteristics of NF6 regular fault, the FLAC3D numerical calculation mannequin is mounted with dimensions of 710 m × 450 m × 180 m. Two numerical calculation fashions are hooked up to examine and analyze the fault slip instability rule and the dynamic response traits of stope underneath different mining influences. One model simulated how the mining of the working face passes over the fault from the hanging wall side, while the other model simulated how it passes over the fault from the footwall side (hereafter referred to as the "HW model" and "FW model" for convenience). Table 1 shows the mechanical parameters of the coal-rock mass in the models. The failure criterion of coal-rock mass was investigated by the use of the Mohr–Coulomb strength criterion the. The simulation of the fault was conducted by the use of a ubiquitous joint model, with its parameters set to 1/5 of the sandstone parameters in the roof strata, because the joints and fractures in the fault zone will reduce these parameters. The tensile strength and dilation angle of the joint were set to 0. The friction angle of fault is generally 21–38°, so the friction angle of the normal fault in this simulation is taken as 30° (Barton and Choubey. 1977). Based on the results of in-situ stress testing, the lateral pressure coefficient along the inclined direction of the fault was taken as 0.6, and the lateral pressure coefficient along the strike direction of the fault was taken as 0.8.

3.2 Dynamic calculation and simulation method of fault slip

Fault slip activation releasing tremendous energy is an essential condition the incidence of fault slip type rockburst, and quantifying the energy released by fault slippage under mining-induced influences is the key to reveal the mechanism of fault slip type impact ground pressure and assess the risk of fault slip impact. The energy released by fault slippage can

Table 1 Mechanical parameters of coal and rock mass

Lithology	E (GPa)	C (MPa)	φ (°)	σ (MPa)	υ	c_r (MPa)	ε_p (%)
Medium sandstone	10.5	3	34.5	0.62	0.22	0.6	0.01
Siltstone	6.7	2.1	31	0.37	0.24	0.42	0.01
Mudstone	2.9	1.2	29	0.2	0.28	0.24	0.01
Coal	1.1	0.9	26	0.12	0.34	0.18	0.01

E is the elastic modulus, C is the cohesion, φ is the friction angle, σ is the tensile strength, υ is the Poisson's ratio, c_r is the residual cohesion, ε_p is the plastic strain when the rock mass strength becomes the residual value.

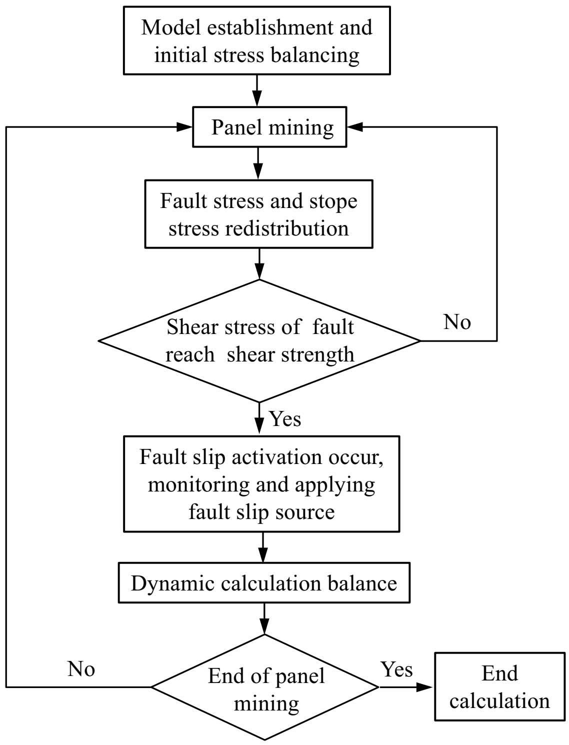

Fig. 3 Numerical calculation flow chart

be characterized in the form of seismic moment M_0, and the equation for calculating seismic moment is 1 (Sainoki et al. 2014).

$$M_0 = GDA \tag{1}$$

Here, G represents the shear modulus of the fault, D represents the fault slip, and A represents the fault shear area.

Numerical simulation is mainly divided into the following steps: Firstly, a numerical calculation mannequin is first installed to stability the preliminary crustal stress. Secondly, the panel is excavated and the fault stress state is monitored. Thirdly, the magnitude of the fault slip source M_0 is calculated. The release pattern of fault slippage energy under different mining conditions is investigated, and dynamic analysis module to apply the seismic moment M_0 due to fault slippage is applied in the form of concentrated moment. This allowes to reveal the dynamic response characteristics of the mining field under the action of fault slip load, and analyzes the dynamic response characteristics of the mining space coal rock body stress field, velocity field, energy field and other fields under the action of fault-slip induced dynamic loads. It is worth noting that when the static calculation is carried out, the boundary around the model and the bottom surface are fixed, and when the dynamic calculation is carried out, the model boundary becomes the quiet boundary. This reveals the mechanism of impact ground pressure induced by fault energy slip load disturbance, and Fig. 3 shows the numerical calculation process.

3.3 Fault slip instability law under mining influence

3.3.1 Characteristics of fault slip

Mining activities near faults may cause slip, which is necessary for releasing energy. In Fig. 4, the shear stress and shear slip displacement contour for the working face mining from footwall via the fault. It can be observed that as it advanced to a distance of 30 m from the fault, the fault within the range of 52–68 m above the coal seam first underwent slip activation, with a maximum slip amount of 0.031 m. The shear stress in the region where the fault slips decreased, releasing tremendous energy. As the working face keeps advancing to the fault position, the fault slip area keeps developing from higher positions to lower positions. The shear stress of the lower fault, which is closer to the coal seam decreases, and energy is gradually released. In the advancement of the working face to the fault position, the fault in the direct top area also undergoes slip activation, and the maximum slip of the fault reaches 0.098 m, which indicates that the fault slip source approaches the mining coal seam as the working face keeps advancing to the fault.

In Fig. 5, it illustrates the contour of shear stress and shear slip displacement for the working face mining from hanging wall via the fault. It can be observed from the figure that compared with the footwall working face mining, the hanging wall working face mining shows a very large difference in both the fault slip amount and the evolution pattern of fault shear stress. In the continuous advancement of the footwall working face towards the fault position, the shear stress on the fault plane of the coal seam roof continuously increases, while the fault remains in a state of energy storage. However, due to the impact of the fault's dip direction, the disturbance induced by the working

Fig. 4 Shear stress and slip of the fault as mining the panel to various positions (FW model)

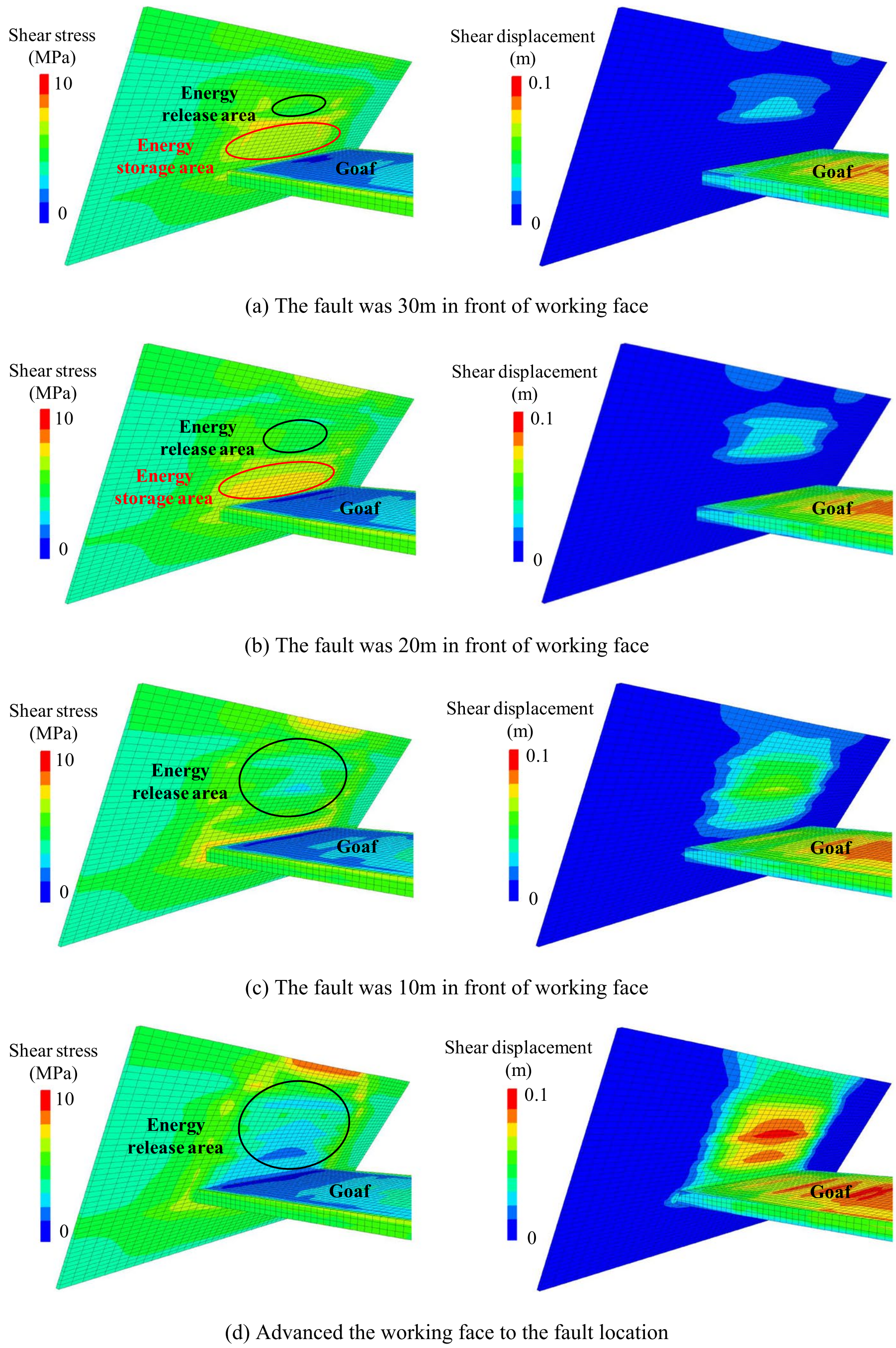

(a) The fault was 30m in front of working face

(b) The fault was 20m in front of working face

(c) The fault was 10m in front of working face

(d) Advanced the working face to the fault location

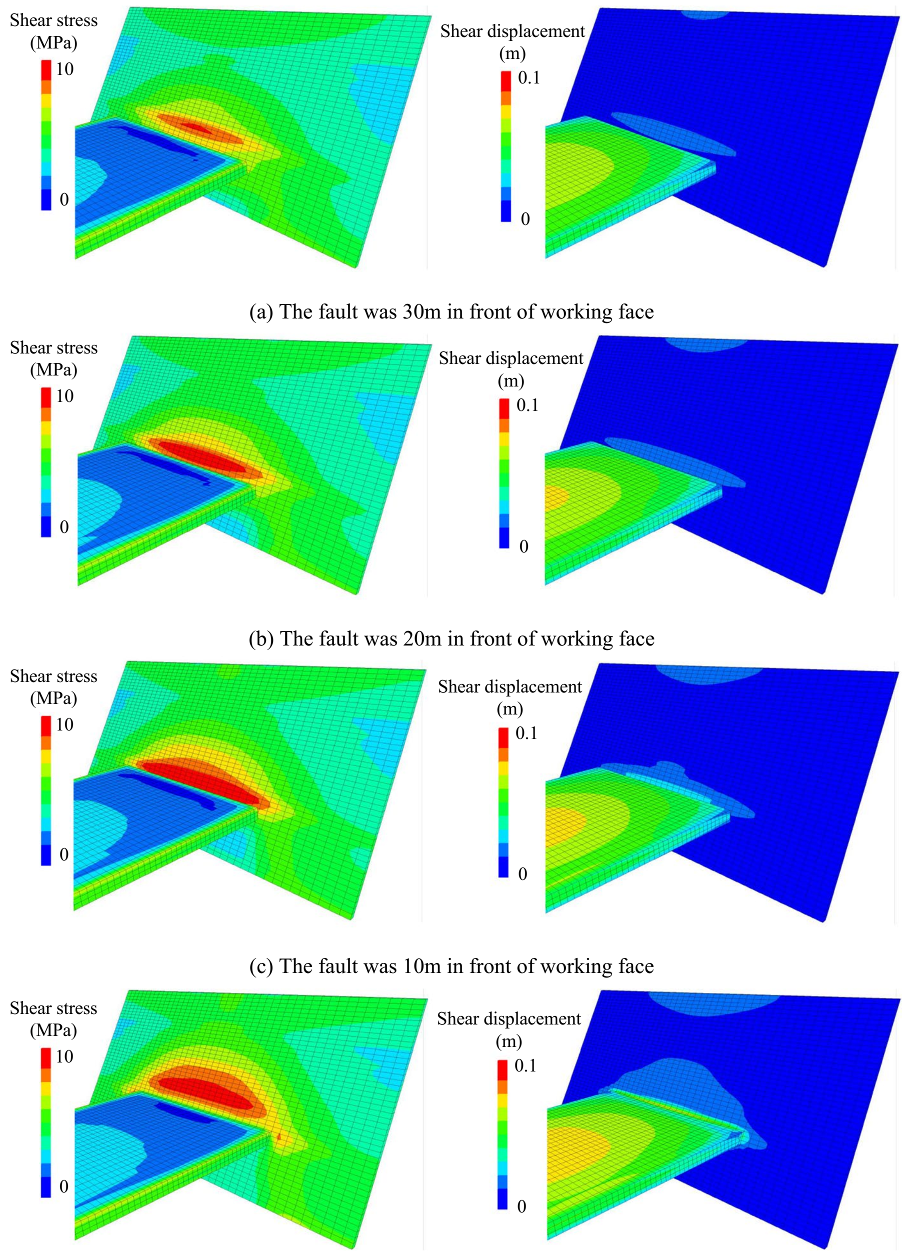

(a) The fault was 30m in front of working face

(b) The fault was 20m in front of working face

(c) The fault was 10m in front of working face

(d) Advanced the working face to the fault location

Fig. 5 Shear stress and slip of the fault as mining the panel to various positions (HW model) face via the fault from hanging wall is incredibly small. Although the shear stress level of the fault surface is high, most of the roof fault areas have not reached the shear strength. Only in the advancement of the working face to the fault position, a small-scale slip occurs in the fault areas close to the coal seam, and the shear stress decreases, releasing the seismic source. The maximum slipping amount of the fault is only 0.023 m. Therefore, when the working face mines via the fault from hanging wall, the working face is less affected by the fault slip dynamic load.

3.3.2 Energy release law of fault slip

Author monitored as well as calculated cumulative seismic moment (M_0) during mining to describe the energy release law of fault slip. The calculation results are presented in Fig. 6. It can be discovered that when the footwall working face mining the fault started out to slip and set off to release energy when the working face used to be 30 m to fault, and the magnitude of seismic moment (M_0) released by fault slip was 2.85×10^{11} N·m. With the working face keeping advancing to distances of 10 m and 0 m from the fault, its slip becomes more intense, and the released energy significantly increases. When the fault was 10 m and 0 m ahead of the working face, the magnitude of M_0 reached 5.19×10^{11} N·m and 9.42×10^{11} N·m. After the working face passed through it, the seismic moment

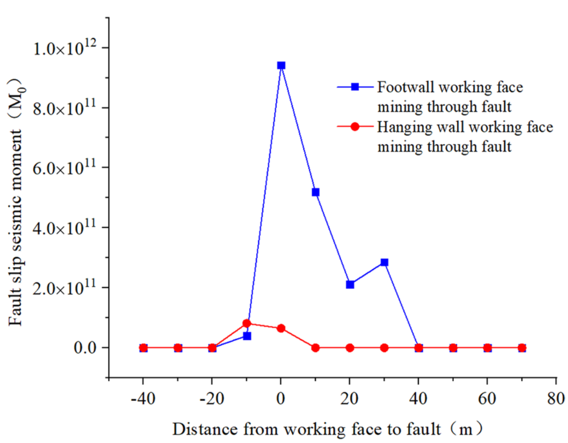

Fig. 6 Seismic moment of fault slip

decreased sharply. The cumulative seismic moment (M_0) associated with fault slip of the footwall working face is noticeably larger than the hanging wall working face. The main reason is that compared to the mining of the hanging wall working face, the mining of the footwall working face result in a more significant reduction in fault stress and a larger sliding range. Consequently, the rockburst hazard is higher when the working face intersects the fault from footwall.

3.4 Dynamic response characteristics of the mining area under disturbance from fault slip

3.4.1 Peak particle velocity of stope

After the fault slip seismic source is launched, stress waves propagate in the surrounding rock mass, causing vibrations in the mining area. The peak particle velocity (PPV) was a significant indicator for the evaluation of the degree of disturbance caused by fault slip seismic source in the mining area. The higher vibration velocity has a significant impact on the stope sorrounding rock as well as the supporting structure, and in severe cases, it can even induce rockburst accidents (Mutke et al. 2015). Therefore, monitoring the stress peak region in the vicinity of the working face and analyzing the vibration velocity during the advancement of the working face can help assess the level of disturbance caused by fault slip seismic source to the surrounding rock mass in the mining area.

In Fig. 7, the vibration velocity of the coal body in the area of the stress peak region when the working face via fault from footwall. The fault slips in the advancement of the working face from 40 to 30 m from the fault (40 m$\geq L \geq$30 m, where L represents how far the working face and the fault is). Because the small range of fault slip induced by mining, the energy released was also small. When the dynamic load caused by fault slip propagates to the coal-rock mass in the stress peak region, the PPV at that position is 0.55 m/s. The duration of dynamic disturbance was relatively short, and the vibration velocity decreased to 0.05 m/s after the dynamic calculation for 0.25 s. In the advancement of working face to a distance of 10 m from the fault, a notable increase

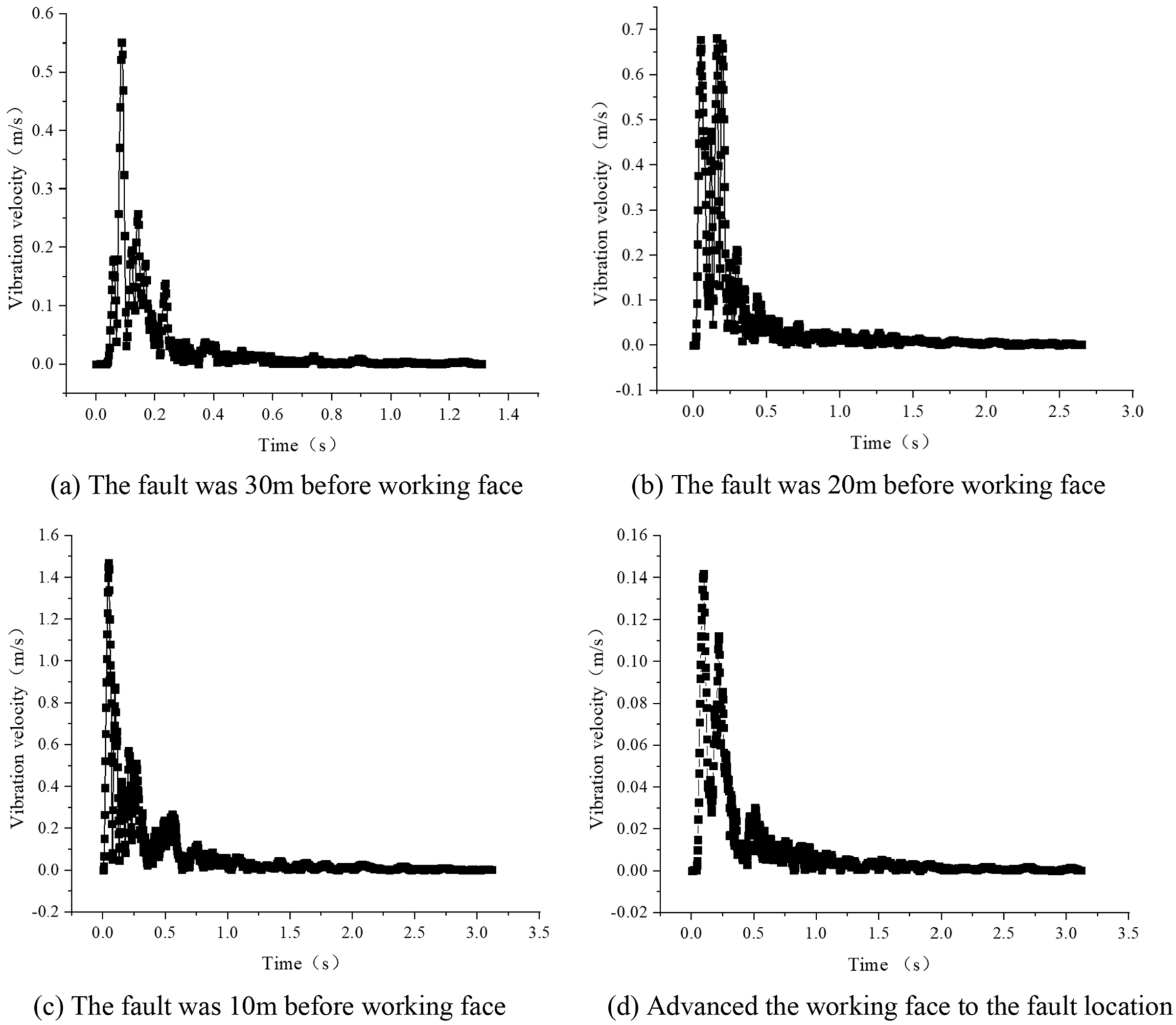

Fig. 7 Vibration velocity at the peak support pressure position when the working face was advanced to different positions

in fault slip seismic activity is observed, accompanied by an elevation in PPV within the stress peak region of the coal-rock mass, reaching 0.68 m/s. When $L=0$ m, the PPV of the stope surrounding rock reached 1.47 m/s, and the vibration duration also significantly increased. When the panel is mined via the fault, the mining doesn't influence the fault, while the PPV significantly decreased to 0.14 m/s.

In Fig. 8, a histogram of the PPV of the coal body in the area of peak support pressure when mining via fault. As can be seen from the histogram, the PPV of the stope was significantly smaller when panel mined via the fault from footwall compared mined via the fault from hanging wall. During the hanging wall panel mining via the fault, the stope's surrounding rockmass experienced only slight vibrations as the panel advanced to the fault position and passed through the fault for 10 m, with the maximum vibration velocity reaching only about 0.4 m/s. Therefore, the surrounding rock of stope was less influenced by fault slip dynamic load as the panel was extracted from the hanging through the fault.

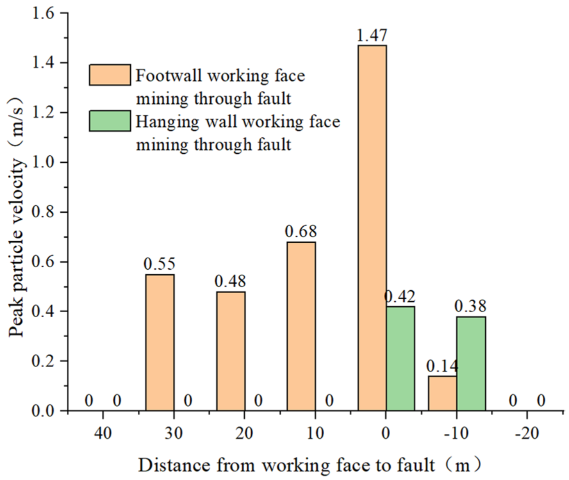

Fig. 8 PPV at peak abutment pressure of stope surrounding rock when the panel advanced to different positions

3.4.2 Dynamic response rule of working face advance abutment stress

The coal mass in the stress peak region of the advanced abutment of the working face accumulates a considerable amount of elastic energy. Under the action of the dynamic stress waves precipitated by way of fault slip, the coal mass in the peak abutment stress region may additionally trip plastic failure and launch a lot of energy, leading to rockburst. Therefore, it is important to monitor the dynamic response law of advance abutment stress at different positions during mining is of great significance for evaluating the rockburst hazard of the working face. In Fig. 9, in the retrieval of working face from footwall over the fault and in its advancement to 20 m from the fault, the highest abutment stress before the action of dynamic load is located at the position of 15 m ahead of the working face. The stress concentration of the coal column is higher due to the fault stress barrier, and the peak abutment stress is as high as 33.1 MPa. The dynamic load causes stress reduction about 20 m, as well as the pressure reduction value of the coal body in highest stress area is 0.2 MPa. When it advances to 10 m from the fault, the peak abutment stress of the working face before the dynamic load is transferred to the coal-rock body area of the footwall, and the peak abutment stress is reduced to 30.5 MPa After the fault slip dynamic load is applied, the impact on abutment stress and the degree of influence increases significantly, and the abutment stress in the 45 m range ahead the working face is reduced, while the highest abutment stress is reduced by 1.1 MPa. When it advances to 0 m from the fault, it causes the abutment stress in the range of 50 m to decrease, and the peak abutment pressure decreases by 5.5 MPa, and the working face's rockburst hazard further increases. When the working face mining viand the fault, the peak abutment stress decreases to 26.2 MPa, while the fault slip dynamic load only causes a little stress in the plastic damage area to decrease, and the coal body at the peak abutment stress area increases slightly.

In Fig. 10, the change pattern of the abutment stress after the dynamic load of mining from the hanging wall via the fault can be seen. By comparing Figs. 9 and 10, it can be considered peak abutment stress affected via the dynamic load of it decreases barely through solely 0.1 MPa, with the working face mined from hanging wall to the fault position. After it passes the fault by 10 m, the impact and fault extent slip dynamic load on the stress of the surrounding rockmass are still small. However, in the highest abutment stress area, fault slip dynamic load makes the stress grow slightly. The dynamic load played a role in energy storage for coal mass. Therefore, while mining via the fault from the hanging wall, the disturbance stress degree caused by dynamic load is significantly lower than that caused by mining from the footwall.

3.4.3 Dynamic response characteristics of elastic energy density in the support pressure peak region of the working face

From Fig. 11, we can see that the characteristics of the dynamic response of the coal rock body elastic energy density (EED) with peak abutment stress, it is at the working face mined to different position. According to Fig. 11(a), when the fault advanced 20 m from the working face, the EED in highest abutment stress area was in the peak. But due to the slight dynamic load of the fault slip, the EED of the coal mass in the peak abutment stress region only decreased 7 kJ/m^3. As the fault was 10 m and 0 m ahead of the working face, the EED in the peak abutment stress region also decreased before the dynamic

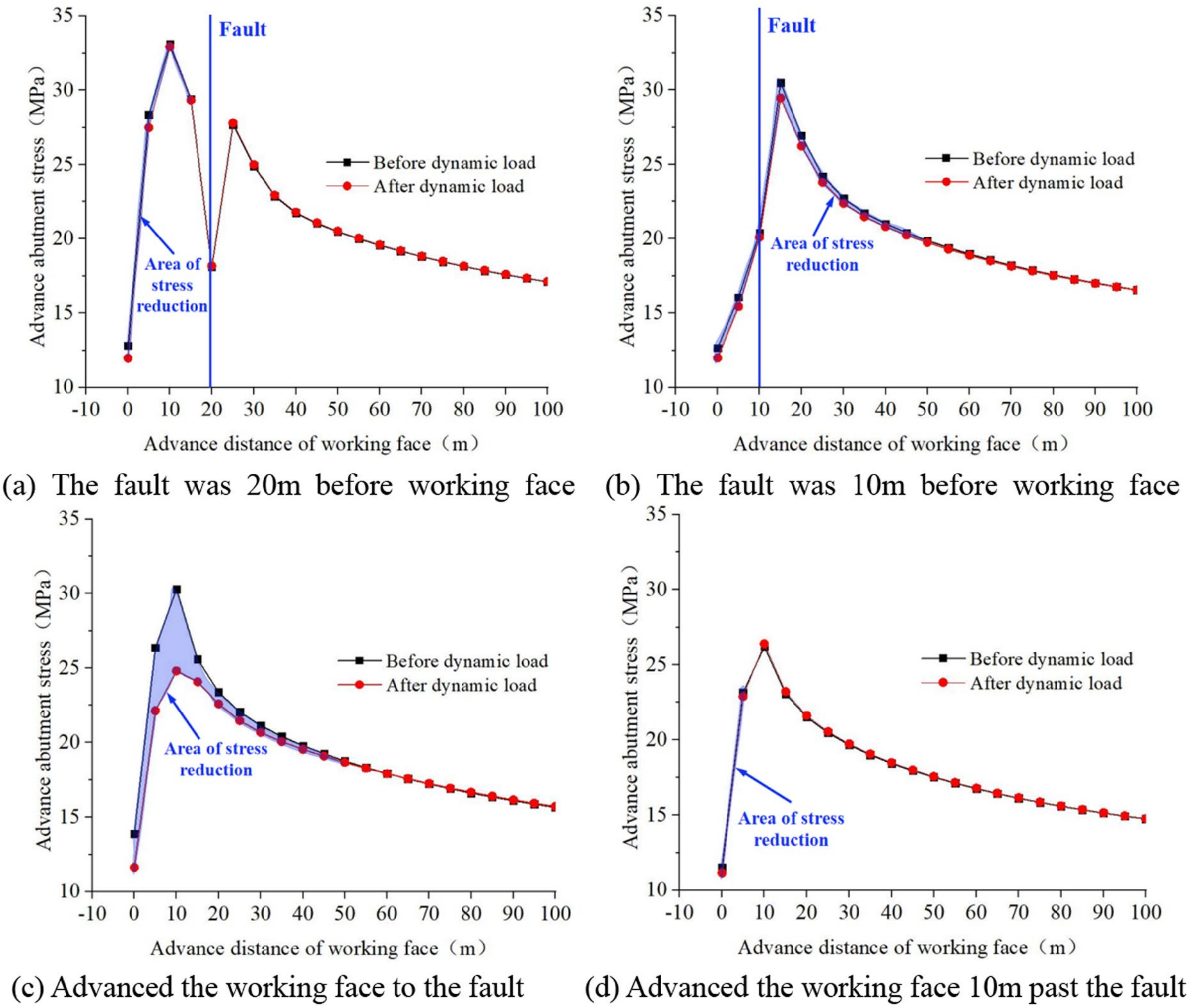

Fig. 9 Dynamic response rule of advanced abutment stress when the panel was mined through fault from footwall

load came into play. However, a strong fault slip dynamic load influences the stope, where the EED of coal mass in the peak abutment stress area decreases significantly. Especially when the working face near the fault, the discount value in EED reached 81 kJ/m^3 and the load transferring substantial plastic harm to coal mass and launching a massive quantity of elastic energy. Therefore, the hazard of rockburst was relatively high.

By comparing Fig. 11(a) and (b), it is evident that the EED of coal and rock body around the hanging wall panel was less affected by fault slip compared with the footwall panel. The EED of peak abutment stress area just changed quitely after the fault slip dynamic load. Therefore, when the panel crossed through fault from the hanging wall, the degree of disturbance of the rock mass EED by the fault slip load was much smaller than if it crossed inversely.

4 Energy condition for initiation of fault slip type rockburst

Rockburst occurs when a lot of elastic energy stored in the coal-rock mass is suddenly and violently released. However, for fault slip type rockburst, the accumulation of elastic energy in the coal rock mass is solely a prerequisite for rockburst occurrence, and the interference of exterior dynamic load is additionally a key element (Askaripour et al. 2022). As the

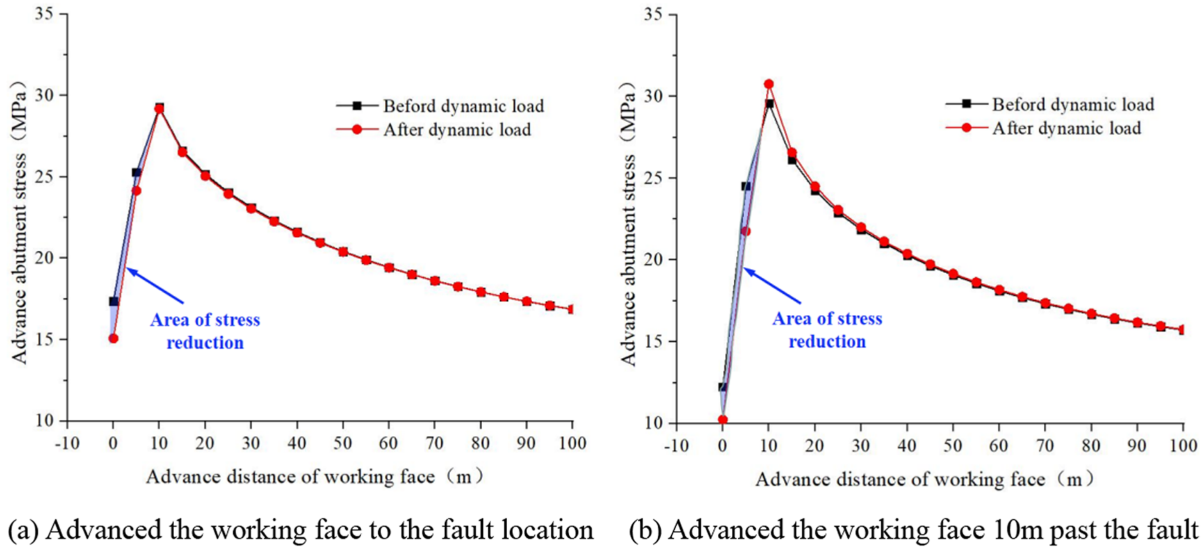

Fig. 10 Dynamic response rule of advanced abutment stress when the panel was mined through fault from hanging wall

working face is retrieved near the fault, the coal body near the stope transitions from a three-way to a unidirectional stress state, resulting in plastic failure and stress redistribution of the surrounding rock stress and the transfer of the working face support pressure to the deep. The coal body in advance of the working face is separated into fracture zone, plastic zone, elastic zone and raw rock stress zone according to the different abutment stress distribution. Among them, the elastic–plastic junction of coal body is subjected to the highest concerntration of abutment stress and accumulates a massive quantity of elastic energy. The fault acts a barrier role in mining stress and a large stress concentration tends to occur in the faulted coal column area. In the propagation of the fault slip dynamic load to the coal mass in the highest stress region, it may cause destabilization of the coal mass. The coal body changes from the elastic to the plastic state, easing abundant elastic vitality so that fault slip type impact ground pressure occurs (Li et al. 2014) (Fig. 12).

4.1 Principle of minimum energy for coal failure

The yield criterion of coal varies depending on its stress state. Under uniaxial stress, the failure criterion of uniaxial compression of coal body is $\sigma > \sigma_c$, and the energy consumed by coal body compression failure is $E_1 = \sigma_c^2/2E$.

The criterion of unidirectional shear failure of coal body is $\tau > \tau_c$, the energy consumed by shear failure of coal body is $E_1 = \tau_c^2/2G$.

Failure criterion of coal under triaxial stress state Mohr–Coulomb criterion (Liu et al. 2020):

$$\sigma_1 = \left[(1 + \sin\varphi)/(1 - \sin\varphi)\right]\sigma_3 + \sigma_c \tag{2}$$

According to the generalized Hooke's theorem, it can be concluded that the elastic strain energy E_0 under the three-way stress state of coal body is (Ning et al. 2017):

$$E_0 = \frac{\left[\sigma_1^2 + \sigma_2^2 + \sigma_3^2 - 2\mu\left(\sigma_1\sigma_2 + \sigma_1\sigma_3 + \sigma_3\sigma_2\right)\right]}{2E_m} \tag{3}$$

where, E_m is elastic modulus, μ is Poisson's ratio,σ_1, σ_2, and σ_3 are all principal stresses.

Coal in a triaxial stress state can accumulate tremendous elastic energy. The coal failure in a triaxial stress has three-dimensional stress failure criterion. However, once coal failure is initiated, the stress state quickly transitions from a triaxial to bi-directional, and ultimately to unidirectional stress. According to the precept of minimal energy for coal failure (Zhao et al. 2003), once a coal body undergoes failure and instability, the strength that needs to be consumed is usually the failure vitality in a unidirectional stress, $E_{f\,min} = \sigma_c^2/2E$ or $E_{f\,min} = \tau_c^2/2G$, and this energy is the least vitality for

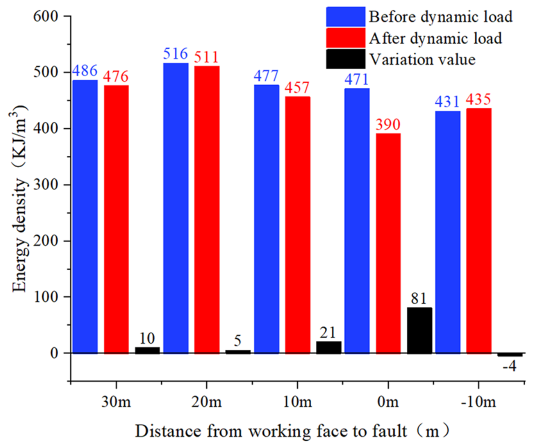

(a) Working face mined via fault from footwall

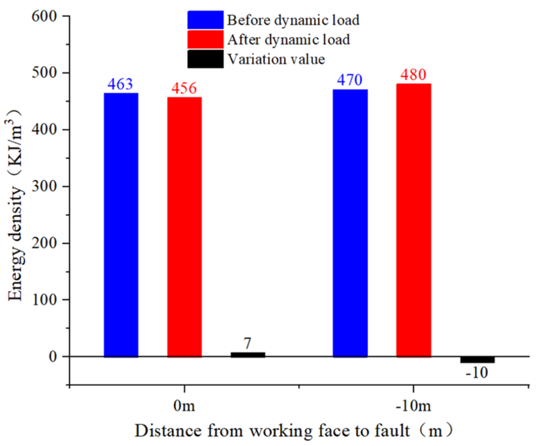

(b) Working face mined via fault from hanging wall

Fig. 11 Energy evolution rule of coal body in the peak advanced abutment stress area under the disturbance of fault slip dynamic load

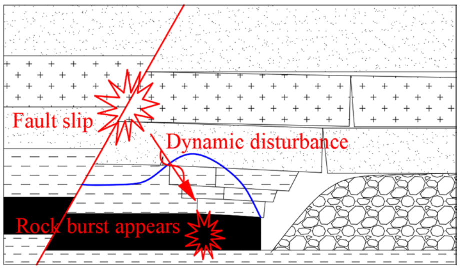

Fig. 12 Schematic diagram of the occurrence mechanism of fault slip rockburst

coal failure. And the difference between elastic energy stored in the 3D stress state of coal and rock mass and minimum failure energy is the elastic residual energy W_C of coal failure, which can be expressed as:

$$W_C = E_0 - E_{fmin} \quad (4)$$

W_C reprents the elastic residual energy of coal failure. In most cases, this electricity is launched in the structure of kinetic energy, which is converted into the ejection of broken coal or strong vibration of coal rock mass. The greater the elastic power of coal in an elastic state, the greater the elastic residual energy during coal failure, and the more severe the impact manifestation.

4.2 Energy criterion for the initiation of fault slip type rockburst

In the same region, the elastic modulus E_m and Poisson's ratio μ can be considered as a fixed value for coal bodies. According to the calculation formula 2 of elastic pressure power of coal body, the elastic power stored in coal body depends on the size of main stress, and he elastic power increases with an extend in stress concentration, so the EED in the restrict equilibrium place of coal body is the largest. According to the precept of minimal strength for coal body failure, regardless of the stress state in which the coal body undergoes failure, the strength required for its failure is the energy consumed under uniaxial conditions. Therefore, when the energy accumulated by the static stress concentration of the coal body in limit equilibrium realm and the energy input by the fault slip load exceed the least vitality needed coal body failure, and the rockburst begins to activate in the limit equilibrium area. After initiation, elastic residual energy causes the coal body in the plastic zone to violently burst out, resulting in the severe manifestation of fault slip type rockburst.

The amount of energy launched by fault slip is influenced by the shear stress drop ($\Delta\tau$), the amount of fault shear displacement (D), and the area of fault slip (A). The quantity of electricity launched with the aid of fault slip is proven in formula 4 (Sainoki et al. 2014). Energy dissipation occurs in the process of dynamic load stress wave propagation to the surrounding area after the source is released by fault slip. Dynamic load propagation in coal and rock mass follows a power function attenuation law. The dynamic load near the source is the largest, and as the distance from the fault increases, the load rapidly decreases. The vitality E_d in the peak pressure region near the working face is shown in formula 6 (Cao et al. 2023):

$$E = \frac{\Delta\tau DA}{2} \tag{5}$$

$$E_d = ER^{-\eta} = \frac{\Delta\tau DAR^{-\eta}}{2} \tag{6}$$

In the equation: R is the distance from the fault slip region to the peak stress region next the face, η is the energy attenuation index of the propagation of dynamic load in rock medium.

From this, it can be conducted that the energy condition of fault slip rockburst initiation is the superposition of the energy in the coal body of top stress vicinity and the load energy transmitted by the fault slip source, which exceeds minimum energy required for coal body failure. Therefore, the energy criterion for the initiation of fault slip type rockburst can be expressed as:

$$E_0 + E_d - E_{f\min} > 0 \tag{7}$$

Bringing formulas 3 and 6 into 7 yields, Coal compression failure:

$$\frac{\left[\sigma_1^2 + \sigma_2^2 + \sigma_3^2 - 2\mu\left(\sigma_1\sigma_2 + \sigma_1\sigma_3 + \sigma_3\sigma_2\right)\right]}{2E_m} + \frac{\Delta\tau DAR^{-\eta}}{2} - \sigma_c^2/2E_m > 0 \tag{8}$$

Coal shear failure:

$$\frac{\left[\sigma_1^2 + \sigma_2^2 + \sigma_3^2 - 2\mu\left(\sigma_1\sigma_2 + \sigma_1\sigma_3 + \sigma_3\sigma_2\right)\right]}{2E_m} + \frac{\Delta\tau DAR^{-\eta}}{2} - \sigma_c^2/2G > 0 \tag{9}$$

The elastic residual energy W_C during the occurrence of fault slip type rockburst can be expressed as:

$$W_C = E_0 + E_d - E_{f\min} \tag{10}$$

Based on the above analysis, fault slip release the magnitude of energy, which together with the static pressure of the coal, are closely related to the initiation and severity of fault slip type rockburst. The potential of rockburst is higher under the combined effect of high static load and strong dynamic load of fault slip. As the working face mining via a fault in the hanging wall or footwall, the difference of static stress in the mining area is relatively small. However, the energy launched by fault slip with the panel mined via fault from footwall is much greater than that from hanging wall, so the potential of rockburst is higher with the panel mining via a fault from hanging wall.

5 Conclusion

This study employed numerical simulation and theoretical analysis to compare the energy release rule during mining the panel through fault from hanging wall and footwall. Its response characteristics of quarry with relative load and criterion for initiation of fault slip rockburst were proposed. Here are some major conclusions about this study:

The energy release rule and dynamic load effect of fault slip were studied based on FLAC3D numerical simulation. The seismic moment (M_0) associated with fault slip during panel mining through the fault from the footwall is valuably greater than that in the mining of the panel through the fault from hanging wall. The slip activation first occurred on the high position fault and as the panel mined to the fault position, the slip activation occurred on the low position fault, releasing more energy than the high position fault.

The fault slip dynamic load produced dynamic load disturbance on the stope, causing significant vibration of the stope surrounding roakmass. As the panel mining from the footwall through the fault, the vibration velocity of stope surrounding roakmass was greater, while the potential of rockburst was higher. Moreover, the coal and rock mass in peak abutment plastic failure occurred with the strong dynamic load of fault slip, and the peak stress significantly decreased, releasing tremendous energy.

Based on energy theory, an energy criterion for the prevalence of fault slip type rockburst was proposed. The initiation and severity of fault slip rockburst are closely related to the magnitude of the energy released by fault slip and the static stress of surrounding rock. The potential of rockburst was higher under the combined effect of high static stress and dynamic load of fault slip.

Author contributions LX and PK contributed equally to this study, and they jointly wrote the main manuscript text. LX and CW are the co-corresponding authors of this work. ML and JH prepared all the figures in the manuscript. ML and CW processed all the data in the manuscript. All authors reviewed the manuscript.

Funding The research for this study used to be subsidized by using the Natural Science Foundation of Anhui Province (2208085QE144), the National Natural Science Foundation of China Youth Program (52304074, 52304198), the Open Fund of Engineering Laboratory for Safe and Precise Coal Mining of Anhui Province (ESCMP202308), the Opening Foundation of Shandong Key Laboratory of Civil Engineering Disaster Prevention and Mitigation, Shandong University of Science and Technology (CDPM2021KF13), the Doctoral Research Fund of Shandong Jianzhu University (XNBS20116), the Key Project of National Natural Science Foundation of China (U21A20110), and the Start-up Fund for Introducing Talents and Scientific Research of Anhui University of Technology (13210151).

Data availability The data that has been used is confidential.

Declarations

Ethics approval and consent to participate Not applicable.

Consent to publish The results/data/figures in this manuscript have not been published elsewhere, nor are they under consideration by another publisher.

Competing interests The authors declare that they have no known competing financial interests or personal relationships that could have appeared to influence the work reported in this paper.

References

Askaripour M, Saeidi A, Rouleau A et al (2022) Rockburst in underground excavations: a review of mechanism, classification, and prediction methods. Undergr Space 7(4):577–607

Avuli M, Karalar M (2021) Three dimensional seismic deformation-shear strain-swelling performance of America–California Oroville earth-fill dam. Geomech Eng 24(5):443–456

Barton N, Choubey V (1977) The shear strength of rock joints in theory and practice. Rock Mech 10(1):1–54

Cai W, Dou LM, Si GY et al (2021) Fault-induced coal burst mechanism under mining-induced static and dynamic stresses. Engineering 7:687–700

Cao MH, Wang TX, Li KS (2023) A numerical analysis of coal burst potential after the release of the fault-slip energy. Rock Mech Rock Eng 56(5):3317–3337

Chen GH, Li XB, Zhang P et al (2016) Dynamic response of rockmass under fault-slip rockburst based on focal mechanism. China Saf Sci J 26(11):121–126

Fan J, Chen J, Jiang D et al (2019) A stress model reflecting the effect of the friction angle on rockbursts in coal mines. Geomech Eng 18(1):21–27

Hu LH, Ma K, Liang X et al (2018) Experimental and numerical study on rockburst triggered by tangential weak cyclic dynamic disturbance under true triaxial conditions. Tunn Undergr Space Technol 81(11):602–618

Jiang LS, Kong P, Zhang PP et al (2019) Dynamic analysis of the rock burst potential of a longwall panel intersecting with a fault. Rock Mech Rock Eng 53:1–18

Kong P, Jiang LS, Shu JM et al (2019) Mining stress distribution and fault-slip behavior: a case study of fault-influenced longwall coal mining. Energies 12(13):2494

Kong P, Xing LY, Xu CW et al (2022) Investigation of shear mechanical behavior and slip weakening characteristics of rough joints in rock mass. Sustainability 14(15):9654–9654

Li ZL, Dou LM, Cai W et al (2014) Investigation and analysis of the rock burst mechanism induced within fault–pillars. Int J Rock Mech Min Sci 70:192–200

Liu X, Ma JW, Tang HM et al (2020) A novel dynamic impact pressure model of debris flows and its application on reliability analysis of the rock mass surrounding tunnels. Eng Geol 273:105694

Mottahedi A, Ataei M (2019) Fuzzy fault tree analysis for coal burst occurrence probability in underground coal mining. Tunn Undergr Space Technol 83:165–174

Mutke G, Dubiński J, Lurka A (2015) New criteria to assess seismic and rock burst hazard in coal mines. Arch Min Sci 60(3):743–760

Ning JG, Wang J, Jiang JS et al (2017) Estimation of crack initiation and propagation thresholds of confined brittle coal specimens based on energy dissipation theory. Rock Mech Rock Eng 51:119–134

Sainoki A, Mitri HS (2014) Dynamic modelling of fault-slip with Barton shear strength model. Int J Rock Mech Min Sci 67:155–163

Su GS, Chen ZY, Yan ZF et al (2021) Experimental study of the dynamically induced rockburst of a rock wall with double free faces. Int J Damage Mech 28(4):611–637

Vardar O, Wei C, Zhang C, Canbulat I et al (2022) Numerical investigation of impacts of geological faults on coal burst proneness during roadway excavation. Bull Eng Geol Env 81(1):1–12

Wang T, Wang ZH, Jiang YD et al (2014) Experimental study of stress distribution and evolution of surrounding rock under the influence of fault slip induced by mining. J China Univ Min Technol 43(4):588–592

Wang GF, Gong SY, Dou LM et al (2018) Rockburst characteristics in syncline regions and microseismic precursors based on energy density clouds. Tunn Undergr Space Technol 81(11):83–93

Wang HW, Shi RM, Song JQ et al (2021) Mechanical model for the calculation of stress distribution on fault surface during the underground coal seam mining. Int J Rock Mech Min Sci 144:104765

Xiao ZM, Gu ST, Zhang YZ et al (2023) An effective control method of rock burst induced by shear instability of fault structure under complicated geological conditions. Bull Eng Geol Env 82(4):1–24. https://doi.org/10.1007/S10064-023-03119-1

Zhao YS, Feng ZC, Wan ZJ (2003) Least energy priciple of dynamical failure of rock mass. Chin J Rock Mech Eng 22(11):1781–1783

Publisher's Note Springer Nature remains neutral with regard to jurisdictional claims in published maps and institutional affiliations.